

Novel Insulator to Metal Transition and Superconductivity in Sr-doped La_2CuO_4

Young Hoon Kim¹ and Pei Herng Hor²

¹ Department of Physics, University of Cincinnati, Cincinnati, Ohio 45221-0011

² Department of Physics and Texas Center for Superconductivity
University of Houston, Houston, Texas 77204-5002

Submitted to Phys. Rev. B

We have studied the charge dynamics of Sr-doped La_2CuO_4 at hole concentration $p = 0.07$. We observed a clear indication of the competition between two Wigner lattice orders: One corresponds to a $T_c = 15$ K superconductivity and the other to $T_c = 30$ K. Our results naturally explain the recent observation of metallic transport in extremely low (1%) Sr-doped La_2CuO_4 and establish a novel insulator to metal transition mechanism and superconductivity in the 2D Wigner lattice ground state. We suggest that the fluctuations of the relative phase between the superconducting condensate and the Wigner lattice order account for the recent observation of the transverse Josephson plasmon mode. PACS Number: 78.30.Er 72.15.-v 74.25.Fy 74.72.Jt

1. Introduction

The superconducting (SC) order in cuprates originates from the two-dimensional (2D) charge dynamics of the doped holes (or electrons) in the CuO_2 planes. The undoped cuprates at half-filling exhibit 2D antiferromagnetic order. Away from half-filling, the SC order sets in as the doping concentration (p) increases beyond the critical hole concentration $p_c = 1/16$ and a generic phase diagram as a function of p and temperature (T) has been constructed using a variety of experimental probes [1]. Therefore, understanding the charge dynamics in the CuO_2 planes away from half-filling is particularly relevant and until our far-infrared (far-IR) study results of Sr/O co-doped $\text{La}_{1.985}\text{Sr}_{0.015}\text{CuO}_{4+\delta}$ systems were published recently [2], no clear physical picture regarding the normal-state low-lying electronic excitations away from half-filling has been given. This has been particularly true of the far-IR studies despite all the relevant energy scales are within the reach of the far-IR probe energies.

We have carried out detailed transport and far-IR reflectivity measurements of a single phase polycrystalline $\text{La}_{1.93}\text{Sr}_{0.07}\text{CuO}_4$ sample for the

frequency range from $\sim 7 \text{ cm}^{-1}$ to 5000 cm^{-1} . We chose $p = 0.07$ system $\text{La}_{1.93}\text{Sr}_{0.07}\text{CuO}_4$ which shows a SC transition at $T_c = 16$ K. This system is chosen to directly compare with the previously obtained data of Sr/O co-doped La_2CuO_4 near $p_c = 1/16$. We chose to study the polycrystalline sample for the following two reasons: (1) There exists a serious problem with uniform distribution of the Sr atoms in preparing single crystalline samples at low doping concentrations and (2) far-IR studies of single crystalline sample is no longer essential because details of the c-axis charge dynamics in cuprates is now understood and the c-axis far-IR spectral information is well-documented.

In this paper, we report the results of our recent charge dynamics studies of 7% Sr-doped La_2CuO_4 superconductor ($p = 0.07$ and $T_c = 16$ K). We have observed a clear indication of competition between the p(4x4) Wigner lattice (or 2D Charge Density Wave) and the c(2x2) lattice order (see Figure 3). We found that, as the c(2x2) lattice order loses the competition, the $T_c = 16$ K superconductivity results unlike the case of $p = 0.07$ Sr/O co-doped counterpart which exhibited $T_c = 26$ K [2]. Our results resolve the problem of

the insulator to metal (I-M) transition in cuprates [3] and establish a novel I-M transition mechanism and superconductivity in the 2D Wigner lattice ground state. The issue of the metallic transport in 1% Sr-doped La_2CuO_4 for $T > 100$ K [4] can be understood based on our findings. The observed phase collective mode in the SC state provides a channel for the coupling of the c-axis polarized far-IR photon field to the fluctuations of the relative phase between the SC condensate and the Wigner lattice order. We believe that this accounts for the recent observation of the mode called transverse Josephson plasmon mode in the c-axis far-IR conductivity [5].

2. Experimental

Far-IR reflectivity was measured at near normal angle of incidence ($\sim 8^\circ$) on the sample. Bruker 113v infrared spectrometer was used. In order to cover the frequency (ω) below 20 cm^{-1} , a 75 micron Mylar beamsplitter and a doped Si-composite bolometer with 1 cm^2 active area operating at 2 K was used in conjunction with a parabolic light cone with a 7 mm diameter exit aperture.

The sample temperature was controlled by direct measurement of the temperature from the backside of the sample. The temperature resolution was ± 0.1 K for $T \leq 40$ K. Far-IR properties, represented by the real part of conductivity $\sigma_1(\omega)$ and the real part of the dielectric function $\epsilon_1(\omega)$, were calculated from a Kramers-Kronig analysis. Spectral resolution was set to 4 cm^{-1} for ω above 600 cm^{-1} , 2 cm^{-1} for $30\text{ cm}^{-1} < \omega < 600\text{ cm}^{-1}$, and 1 cm^{-1} for $\omega < 30\text{ cm}^{-1}$.

3. Results and Discussions

Far-IR and infrared reflectivities of $\text{La}_{1.93}\text{Sr}_{0.07}\text{CuO}_4$ sample at various T are displayed in Figure 1. There appears a sharp minimum in the reflectivity at $\omega \sim 16\text{ cm}^{-1}$ below which the reflectivity curve resembles that of a free electron gas. Above this ω edge, three modes are present: one at $\sim 24\text{ cm}^{-1}$, a weak mode at $\sim 46\text{ cm}^{-1}$, and the third at $\sim 100\text{ cm}^{-1}$ in addition to the c-axis phonon modes at $\sim 230\text{ cm}^{-1}$, \sim

310 cm^{-1} , and $\sim 500\text{ cm}^{-1}$. This 500 cm^{-1} mode is also present in the in-plane spectrum. Because of the highly featureless, insulating nature of the c-axis spectrum even for the optimally doped single crystals, one may safely conclude that the observed spectral features other than the c-axis phonons are from the CuO_2 planes.

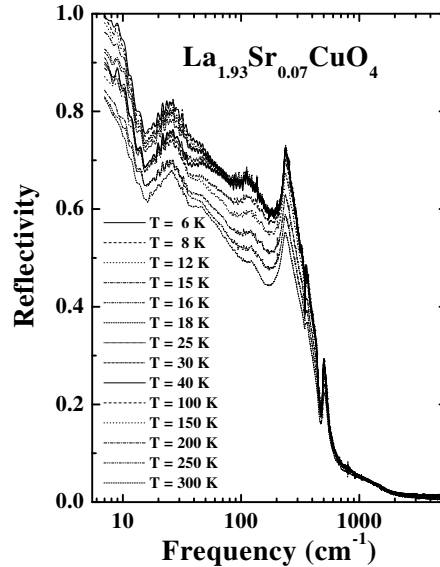


Figure 1. Far-infrared and infrared reflectivity spectra of polycrystalline $\text{La}_{1.93}\text{Sr}_{0.07}\text{CuO}_4$ at various temperatures.

The Kramers-Kronig transformation derived $\sigma_1(\omega)$ and $\epsilon_1(\omega)$ are shown in Figure 2. A number of peaks appear in $\sigma_1(\omega)$. Besides the well-known c-axis and in-plane phonon modes, a sharp peak at $\sim 24\text{ cm}^{-1}$ and a broad peak at $\sim 100\text{ cm}^{-1}$ and weak modes at $\sim 46\text{ cm}^{-1}$ and at $\sim 70\text{ cm}^{-1}$ are readily seen and the oscillator strength of these modes show T-dependence. A relatively T-independent broad excitation peaked at $\sim 1200\text{ cm}^{-1}$ with an onset at $\sim 400\text{ cm}^{-1}$ is clearly seen. In addition, there exists a sharp upturn in $\sigma_1(\omega)$ for $\omega < 10\text{ cm}^{-1}$.

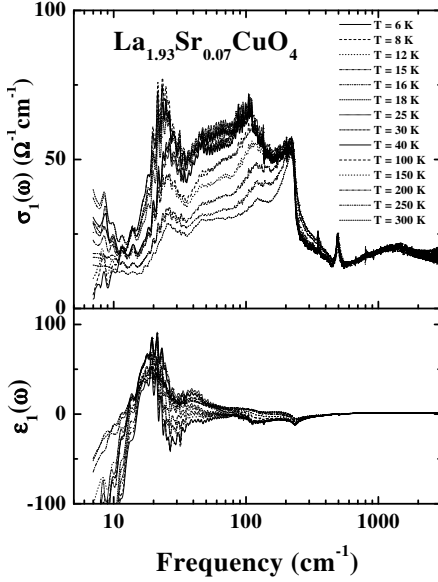


Figure 2. The real part of the conductivity $\sigma_1(\omega)$ (upper panel) and the corresponding real part of the dielectric function $\epsilon_1(\omega)$ (lower panel) calculated via the Kramers-Kronig transformation of the reflectivity.

In our recent far-IR studies of $\text{La}_{1.985}\text{Sr}_{0.015}\text{CuO}_{4+\delta}$ samples at the hole concentration $p \sim 0.063$ ($\delta = 0.024$) and $p \sim 0.07$ ($\delta = 0.032$) [2], two 2D Wigner lattice orders were proposed as the ground state of the CuO_2 plane away from half-filling. We observed that, at $p = 0.063$, almost all the holes are spent to form a $p(4 \times 4)$ square lattice ($p_c = 1/16$) of side $L = 4a$ ($a = \text{Cu-Cu distance}$) as depicted in Figure 3. At $p = 0.07$, a new 2D Wigner lattice order coexisting with the $p(4 \times 4)$ lattice was found and a $T_c = 26$ K was observed. This new 2D Wigner lattice order has $c(2 \times 2)$ symmetry ($p_c = 1/8$, $L = 2\sqrt{2}a$) (see Figure 3) and is responsible for a $T_c = 30$ K superconductivity. These new 2D Wigner lattice ground states were identified by the presence of the Goldstone mode resulting from the broken translational symmetry. The $\omega = 0$ Goldstone mode (ω_G) of the Wigner lattice

has been shifted to $\omega_{GL} \sim 23 \text{ cm}^{-1}$ for $p(4 \times 4)$ lattice and to $\omega_{GH} \sim 46 \text{ cm}^{-1}$ for $c(2 \times 2)$ lattice due to the commensuration pinning of the Wigner lattice to the underlying CuO_2 lattice.

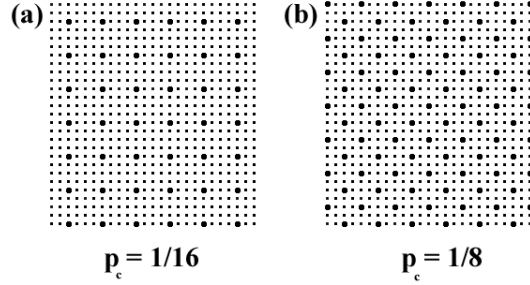


Figure 3. Two-dimensional square Wigner lattice diagram. (a) $p(4 \times 4)$ lattice and (b) $c(2 \times 2)$ lattice. The smaller dots represent the copper sites. The larger dots indicate the sites occupied by the electrons (or holes).

The presence of the 2D Wigner lattice in cuprates plays a profound role in two important ways: (1) Because of the on-site Coulomb repulsion at the lattice sites, the excess holes added to the lattice would occupy the upper-Hubbard band if the charge motion is restricted only to the lattice sites. However, in a square lattice, an excess hole can find an energetically favored location at the center of the square lattice. Moreover, the excess holes ($\Delta p = p - p_c$) placed in the local potential minimum can now have an access to a periodic harmonic potential in the directions to the neighboring identical energy minima. This causes the zero point energy of the excess holes to broaden into a band. The width is dependent on the carrier density in the band. This band (Coulomb band) is gapped by the Coulomb energy (ΔE_c) above the ground state and the excess carriers are delocalized and transport charges coherently. We found that extremely small fraction of holes ($\sim 0.4\%$ of $p = 0.063$, for example) participated in a coherent charge transport and su-

perconductivity. (2) The screening provided by the 2D WL radically influences the charge dynamics of the free carriers in the Coulomb band by providing a frequency region where the interaction energy between two electrons becomes negative. Therefore, once the long-range order of the lattice has been established, the free carriers in the Coulomb band are innately paired at temperatures below a crossover T_o .

In light of our previous studies, we identify the $\sim 24 \text{ cm}^{-1}$ mode with the Goldstone mode (ω_{GL}) of the p(4x4) lattice formed in $\text{La}_{1.93}\text{Sr}_{0.07}\text{CuO}_4$ and the $\sim 100 \text{ cm}^{-1}$ peak with the transitions involving the accompanying Coulomb band (ω_{CL}). This observation suggests that the Coulomb band gap ΔE_c is of the order of $\sim 300 \text{ cm}^{-1}$ with the full band width, $W_c \sim 200 \text{ cm}^{-1}$ (0.025 eV). This observed width W_c gives a density of states at the Fermi energy on the order of $N(0) \sim \Delta p / (W_c/2) \sim 0.15 \text{ states/eV}$. This gives rise to the Pauli susceptibility (χ_p). Therefore, we anticipate the contribution of χ_p to the total susceptibility whenever carriers are present in the Coulomb band. We believe that the peculiar presence of χ_p even at $p = 0.05$ doping [6] is due to this reason. The presence of the Coulomb band is also responsible for the incomplete closure of the single particle excitation gap known as the in-plane pseudogap [7].

From the $\epsilon_1(\omega)$ plot, it is clear that the reflectivity minimum at $\sim 16 \text{ cm}^{-1}$ arises from the zero crossing of the $\epsilon_1(\omega)$ and there is no sign of the related structure seen in the $\sigma_1(\omega)$. Therefore, we assign the reflectivity minimum as the plasma edge which gives the screened plasma frequency of the free carriers $\omega_p \sim 16 \text{ cm}^{-1}$. By assuming the carrier mass be the free electron mass and using the static dielectric constant $\epsilon_1(0) \sim 40$ estimated from $\epsilon_1(\omega)$, we find the free carrier concentration $n_F \sim 2.3 \times 10^{17} \text{ carriers/cm}^3$ which is only 0.43% of the total doped carriers. These free carriers reside in the Coulomb band and are also responsible for the metallic behavior indicated by the sharp upturn in $\sigma_1(\omega)$ below $\omega \sim 10 \text{ cm}^{-1}$ and the negative $\epsilon_1(\omega)$ for $\omega < \omega_p$. This suggests that the charge transport is coherent and nearly dissipationless as the extremely small relaxation rate ($< 4 \text{ cm}^{-1}$) indicates. Notice that the free carrier

plasma frequency remains unchanged with T (see Figure 1) since the screening of the charge is also enhanced as the long range order of the Wigner lattice order develops.

A direct comparison of the $\sigma_1(\omega)$ plot with that of the previously reported $\text{La}_{1.985}\text{Sr}_{0.015}\text{CuO}_{4.032}$ sample ($p = 0.07$) is displayed in Figure 4. The one-to-one correspondence of each mode in two different samples is marked. Note that even at the same hole concentration $p = 0.07$, the $\sim 46 \text{ cm}^{-1}$ and $\sim 70 \text{ cm}^{-1}$ modes of $\text{La}_{1.93}\text{Sr}_{0.07}\text{CuO}_4$ sample are much weaker than the corresponding modes of $\text{La}_{1.985}\text{Sr}_{0.015}\text{CuO}_{4.032}$ sample. At 300 K, the magnitude of the overall far-IR $\sigma_1(\omega)$ is comparable for both $\text{La}_{1.93}\text{Sr}_{0.07}\text{CuO}_4$ and $\text{La}_{1.985}\text{Sr}_{0.015}\text{CuO}_{4.032}$ samples. As T is lowered, it becomes clear that the width of the ω_{GL} of $\text{La}_{1.93}\text{Sr}_{0.07}\text{CuO}_4$ sample is about as twice broad as that of $\text{La}_{1.985}\text{Sr}_{0.015}\text{CuO}_{4.032}$ sample while the strength of the ω_{CL} remains comparable. This implies that the correlation length of the p(4x4) lattice in $\text{La}_{1.93}\text{Sr}_{0.07}\text{CuO}_4$ is about a half of that in $\text{La}_{1.985}\text{Sr}_{0.015}\text{CuO}_{4.032}$.

The T-dependence of the oscillator strength of each mode is shown in Figure 5, the oscillator strength of the $\omega_{GL} \sim 24 \text{ cm}^{-1}$ goes through two changes. There is a relatively abrupt increase in the oscillator strength at $T \sim 180 \text{ K}$ and the other at $T \sim 16 \text{ K}$. However, the $\omega_{GH} \sim 46 \text{ cm}^{-1}$ and the Coulomb band transition ω_{CH} exhibit a peculiar T-dependence. First, they do not show the abrupt increase at $T \sim 200 \text{ K}$ as seen in the $\text{La}_{1.985}\text{Sr}_{0.015}\text{CuO}_{4.032}$ sample. Second, as the ω_{CH} mode loses its oscillator strength below $T \sim 30 \text{ K}$, the oscillator strength of ω_{GH} mode abruptly drops at $T \sim 30 \text{ K}$ indicating no development of the $T_c = 30 \text{ K}$ SC phase collective mode. The $T \sim 180 \text{ K}$ jump of the ω_{GL} is an indication of the development of long-range order of the p(4x4) lattice at $T_o \sim 180 \text{ K}$ as also evidenced by the change of the dynamic mass of the lattice from $m^* \sim 75 m_e$ at 300 K to $m^* \sim 40 m_e$ at 130 K [8]. At the same time, the abrupt increase in the oscillator strength of the Coulomb band transition ω_{CL} at around $T \sim 200 \text{ K}$ suggests that more of the free carriers in the single particle excited state of the Wigner lattice occupy the Coulomb band as temperature is lowered. How-

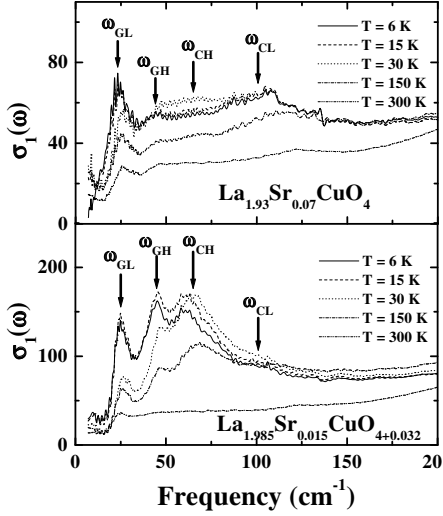


Figure 4. A direct comparison of the $\sigma_1(\omega)$ of $\text{La}_{1.93}\text{Sr}_{0.07}\text{CuO}_4$ with that of $\text{La}_{1.985}\text{Sr}_{0.015}\text{CuO}_{4.032}$ at selected temperatures. (See the text for the notation) Notice the splitting in the peak of the Coulomb band transition in the $c(2 \times 2)$ lattice (ω_{CH}) of $\text{La}_{1.985}\text{Sr}_{0.015}\text{CuO}_{4.032}$ (lower panel). One at $\sim 70 \text{ cm}^{-1}$ is due to the transition from the Coulomb band to the single particle excited state and the other at $\sim 62 \text{ cm}^{-1}$ due to the transition from the ground state to the Coulomb band. The apparent splitting is caused by the relative oscillator strength changes at low temperature.

ever, it appears that the $c(2 \times 2)$ lattice does not develop the long-range order.

This competition is clearly seen in the $d\rho/dT$ plot in Figure 6. While the $d\rho/dT$ of $\text{La}_{1.985}\text{Sr}_{0.015}\text{CuO}_{4.032}$ sample shows a minimum at $\sim 200 \text{ K}$ and a maximum at $\sim 150 \text{ K}$, the $d\rho/dT$ of $\text{La}_{1.93}\text{Sr}_{0.07}\text{CuO}_4$ curve does not show such changes. The subtle changes in ρ amplified by $d\rho/dT$ in $\text{La}_{1.985}\text{Sr}_{0.015}\text{CuO}_{4.032}$ indicate that as the long-range order of the both lattices develops, increase in the number of carriers in the Coulomb band and in their mobility occur and, hence, the corresponding resistivity changes are

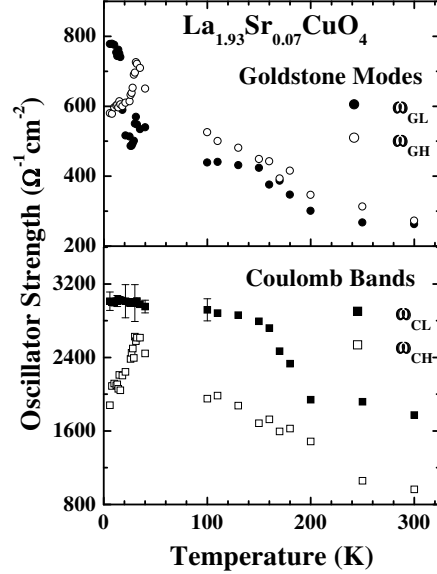


Figure 5. Temperature dependence of the oscillator strengths of the Goldstone modes and the oscillator strengths of the corresponding Coulomb bands. Each oscillator strength was calculated by fitting the $\sigma_1(\omega)$ with a simple symmetric Gaussian as an approximation even though non-trivial asymmetry was evident.

resulted. This tendency is missing in the $d\rho/dT$ curve of $\text{La}_{1.93}\text{Sr}_{0.07}\text{CuO}_4$ owing to the short-ranged domains of the $c(2 \times 2)$ lattice embedded in the $p(4 \times 4)$ lattice. The subtle changes observed in $d\rho/dT$ of $\text{La}_{1.985}\text{Sr}_{0.015}\text{CuO}_{4.032}$ sample have been wash out. This is because the development of the long-range order is inhibited by the frustration of holes due to the Coulomb binding of the holes with the randomly distributed immobile Sr counter-ions. In contrast, the development of long range order of both lattices in $\text{La}_{1.985}\text{Sr}_{0.015}\text{CuO}_{4+0.032}$ sample is enhanced by the mobile intercalated oxygen atoms. This is consistent with the fact that the correlation length of the $p(4 \times 4)$ lattice in $\text{La}_{1.93}\text{Sr}_{0.07}\text{CuO}_4$ is about a half of that in $\text{La}_{1.985}\text{Sr}_{0.015}\text{CuO}_{4.032}$. We found that the short correlation length of the

$c(2 \times 2)$ lattice remains unchanged and only the $p(4 \times 4)$ lattice order develops the long-range order enough to support the $T_c = 16$ K superconductivity in $\text{La}_{1.93}\text{Sr}_{0.07}\text{CuO}_4$.

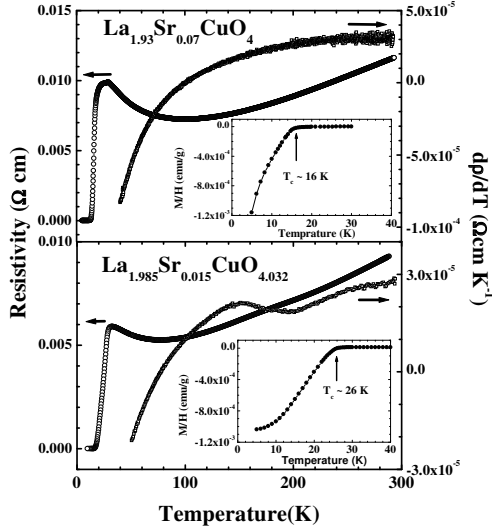


Figure 6. Resistivity and first derivative of the resistivity versus T curves of $\text{La}_{1.93}\text{Sr}_{0.07}\text{CuO}_4$ (upper panel) and $\text{La}_{1.985}\text{Sr}_{0.015}\text{CuO}_{4.032}$ (lower panel). The inset in each panel depicts the Meissner effect. The arrow defines the onset of the superconducting transition temperature (T_c).

2D Wigner lattice formation in a 2D electron gas (2DEG) is a general phenomenon. This has been known for 2DEG on liquid helium surface [9] and in Si MOSFET [10] and GaAs/ $\text{Al}_x\text{Ga}_{1-x}\text{As}$ structures [11] at $B = 0$. The melting criteria for the lattice is given by considering the ratio of the Coulomb energy to the Fermi energy of the 2DEG, r_s given by $r_s = 2m^*e^2 / \epsilon_0 \hbar^2 (\pi n_W / d_\perp)^{1/2}$ where n_W is the carrier density of the Wigner lattice and d_\perp is the interlayer spacing. A Monte Carlo simulation for an ideally clean 2DEG found that the critical value

for the Wigner crystallization of a 2DEG is $r_s = 37 \pm 5$ [12]. This limit tends to decrease as the degree of disorder increases [13]. The lattice vibration and total energy calculation [14] showed that a 2D triangular lattice is favored over a square lattice for the same reason as a simple cubic lattice is unstable against shear when the electrons interact via central forces only.

However, we propose that 2D square Wigner lattice is the ground state charge configuration in the CuO_2 planes away from half-filling. This is because of the symmetry of the underlying CuO_2 lattice and the strong electron-phonon coupling [15] which locks in the electrons to the lattice sites and further lowers the total energy. For a $p(4 \times 4)$ lattice in cuprates, with $n_W \sim 4.4 \times 10^{13}$ carriers/ cm^2 and $m^* \sim 40m_e$, we obtain $r_s \sim 200$, far greater than the critical r_s . Therefore, the lattice ground state is robust until the reduction of the dynamic mass, resulting from the increasing correlation length of the lattice, reaches the threshold beyond which a melting transition should occur. For instance, reducing the dynamic mass of the $c(2 \times 2)$ lattice ($p = 1/8$) to $m^* \sim 10 m_e$ would give $r_s \sim 35$. Thus, at lower doping concentrations below $p = 1/8$, we anticipate the formation of a series of square lattices in the CuO_2 planes as p starts to increase above zero. In fact, indications of such electronic instabilities at preferred p values have been found in a recent Sr/O co-doping studies [16].

The gap in the Goldstone mode at a finite ω in the Wigner lattice plays an important role on the superconductivity in cuprates. This gap gives the dielectric function of the Wigner lattice $\epsilon_1^W(q \rightarrow 0, \omega) = 1 + 4\pi n_W e^2 / m^* (\omega_G^2 - \omega^2)$. Since the Coulomb band is tied to the Wigner lattice, the free carriers in the Coulomb band oscillate in phase with the underlying Wigner lattice at ω_G . Then, there develops a region in ϵ_1^W where the interaction between two electrons, $V = 4\pi e^2 / q^2 \epsilon_1^W(q, \omega)$ becomes attractive ($V < 0$) in $q \rightarrow 0$ limit for $\omega_G < \omega < (\omega_o^2 + \omega_G^2)^{1/2}$, $\omega_o^2 \equiv 4\pi n_W e^2 / m^*$. Therefore, all the free carriers in the Coulomb band are expected to form non-retarded, spin singlet pairs for $T < 180$ K which corresponds to $\omega_o \sim 130 \text{ cm}^{-1}$ estimated from $\epsilon_1(\omega)$. Only when $\omega > \omega_o$ (or $T > 180$ K), these

pairs of electrons dissociate through the Coulomb repulsion. Hence, we identify the crossover $T_o \sim 180$ K as the pairing temperature.

SC order requires not only the spin singlet pairing of electrons but also the long range phase coherence of the SC order parameter, $\psi \sim \Delta e^{i\phi}$. Unlike the conventional BCS superconductors, the phase stiffness energy for cuprates is known to be much smaller [17]. Hence, the phase coherence of the pairs would develop at a T_c substantially lower than the pairing T_o . This point has been experimentally demonstrated by Corson et al. [18] and Xu et al. [19]. Once the phase coherence has been established, there exists the phase collective mode (ω_ϕ) resulting from the broken gauge symmetry. By following the Nambu formalism [20] and incorporating the screened Coulomb interaction in the Wigner lattice ground state, we find $\omega_\phi \approx \omega_G / (1 + \gamma)^{1/2}$ with $\gamma \equiv n_W m_e / n_F m^*$ (n_F = free carrier density) [2]. Hence, the observed abrupt increase in the oscillator strength of the $\omega_{GL} \sim 24$ cm^{-1} mode is due to the development of the ω_ϕ nearly at the same frequency as ω_G [21].

The existence of the phase collective mode at $T \leq T_c$ has a profound effect on the c-axis charge dynamics. We propose that the presence of this phase collective mode manifests itself in the c-axis far-IR $\sigma_1(\omega)$ by inducing a mode arising from small fluctuations of the relative phase between the SC condensate and the Wigner lattice order. Such an idea was originally proposed by Leggett for a two band model superconductor [22]. This mode arises from the dipole moment polarized along the c-axis. Therefore, a peak in the c-axis $\sigma_1(\omega)$ is expected (ω) at $T < T_c$ in addition to the longitudinal Josephson plasmon which solely arises from the zero crossing in the c-axis ϵ_1 [23–26]. We believe that the unidentified 42 cm^{-1} mode in the c-axis $\sigma_1(\omega)$ of $\text{La}_{2-x}\text{Sr}_x\text{CuO}_4$ ($T_c = 34$ K) observed by Basov et al. [27] and the mode at ~ 50 cm^{-1} in $\text{La}_{1.84}\text{Sr}_{0.16}\text{CuO}_4$ ($T_c = 34$ K) [23] and in $\text{La}_{1.85}\text{Sr}_{0.15}\text{CuO}_4$ ($T_c = 35$ K) [24] are direct result of the coupling of the far-IR photon field to the fluctuations of the relative phase of the two condensates. We point out that the recently observed transverse Josephson plasmon mode in the c-axis $\sigma_1(\omega)$ of T^* -phase cuprate

superconductors [5] has the same physical origin and is not unique to the T^* -phase cuprates.

Since the formation of a series of square lattices of holes is favored in the CuO_2 planes as p starts to increase above zero, electrical conductivity with high mobility is expected in cuprates at elevated T whenever there exist carriers in the Coulomb band of each Wigner lattice order. Ando *et al.* [4] recently reported that the mobility of the conducting carriers even in 1% Sr-doped La_2CuO_4 is only a factor of three smaller than that of the optimally doped one at $T \geq 100$ K. Because the mobility is governed by the band width which increases with the carrier concentration in the Coulomb band, we believe the result of Ando *et al.* is a direct consequence of the $p(10 \times 10)$ Wigner lattice formation and the presence of the Coulomb band at $p \sim 0.01$. However, as T decreases, the excess carriers are expected to be localized at a lattice site, which would lead to increasing correlation length of the lattice or to the formation of a different square lattice. Hence, in $T \rightarrow 0$ limit, the system with $p \leq p_c = 1/16$ is an insulator. For a pure Sr-doped La_2CuO_4 , the 2D I-M transition in the Wigner lattice ground state occurs when the free carriers start to occupy the Coulomb band of the $p(4 \times 4)$ lattice for $p > p_c = 1/16$ beyond which the free carriers are paired and the system exhibits the superconductivity.

Studies of the I-M transition in cuprates with Zn-doping or by applying strong magnetic field provide an important test ground for the idea of incipient pairing of electrons below T_o . At the I-M transition, the resistivity is expected to approach the universal critical 2D resistance $\rho_c^{2D} = h/4e^2 \cong 6.5$ k Ω per CuO_2 layer. Indeed, this has been observed in Zn-doped cuprates where $\rho_{I-M}^{2D} \sim 6.8$ k Ω per CuO_2 layer was found [3a, 3b]. In this new type of metal insulator transition, the Mott I-M transition criterion $k_F \ell \sim 1$ (k_F = Fermi wave vector and ℓ = electron mean free path) is no longer valid. The observed unusual value of $k_F \ell \approx 13$ at the I-M transition boundary under strong magnetic field is a direct evidence for this type of novel I-M transition [3c].

We propose that the $c(2 \times 2)$ lattice starts to develop as the hole doping increases beyond $p_c = 1/16$ and at $p_c = 1/8$, the entire CuO_2 plane con-

tains only the $c(2 \times 2)$ Wigner lattice. Because the Coulomb interaction energy of a square lattice per electron is $E_c \cong -0.390e^2/L$ [14], the interaction energy difference δE_c between $p(4 \times 4)$ and $c(2 \times 2)$ lattices is $\delta E_c = -0.404 e^2/a$ per electron. Therefore $c(2 \times 2)$ lattice formation is favored when the Coulomb energy of the electrons in the Coulomb band of the $p(4 \times 4)$ lattice exceeds δE_c . In $\text{La}_{1.93}\text{Sr}_{0.07}\text{CuO}_4$, although both $p(4 \times 4)$ and $c(2 \times 2)$ lattices were found, the long-range order of the $c(2 \times 2)$ lattice could not develop due to the frustration of holes as observed in this work, hence no 30 K superconductivity was obtained. In this context, the observed T_c ranging between 15 K and 30 K for $1/16 < p < 1/8$ would be due to the proximity effect involving the $c(2 \times 2)$ lattice of $T_c = 30$ K and the $p(4 \times 4)$ lattice of $T_c = 15$ K.

Beyond $p = 1/8$, all the additional carriers are expected to occupy the Coulomb band. Then, at the optimal doping ($p \sim 0.16$), the free carrier plasma frequency corresponding to $\Delta p \sim 0.035$ (or $n_F \sim 3.5 \times 10^{20}$ carriers/cm³) becomes $\omega_p = (4\pi n_F e^2 / \epsilon_\infty m_b)^{1/2} \sim 6300 \text{ cm}^{-1}$ ($\sim 0.8 \text{ eV}$) with the electron band mass $m_b \sim 0.2m_e$ and $\epsilon_\infty \sim 2$. Similar values of ω_p were found in Sr- [28,29] and O-doped [30] samples at the optimal doping. Their observed ω_p is much smaller than ω_p calculated by considering entire $p = 0.16$ carriers. In this work, we have found the reason for the discrepancy between the observed ω_p and the calculated ω_p . Because only the carriers in the Coulomb band (Δp) undergo the SC transition ($\Delta p/p = 0.035/0.16 \sim 0.21$), our model provides a natural answer to the question why only $\sim 1/5$ of the total carriers participate in the superconductivity [31]. Also, the T_c will increase as the frequency of the Goldstone mode increases resulting from the reduction in the dynamic mass of the lattice until it reaches the maximum T_c .

We propose that the optimum doping concentration $p \sim 0.16$ is the critical point beyond which the excess carriers gain energy by occupying the $d_{3z^2-r^2}$ orbitals. In the electrochemical doping study of La_2CuO_4 [32], a chemical potential barrier higher than $\sim 1.0 \text{ eV}$ was observed at $p \sim 0.16$. Beyond this point oxygen evolution occurs [32], hence no further doping was achieved. Based

on the optical studies of La_2CuO_4 , it has been suggested by Perkins et al. [33] that the $\sim 0.5 \text{ eV}$ absorption peak in the conductivity is due to the d - d^* exciton formed by promoting a hole from $d_{x^2-y^2}$ to $d_{3z^2-r^2}$. This symmetry forbidden transition is made weakly allowed in cuprates. This peak is also seen in the photoinduced absorption studies [15] and is $\sim 0.5 \text{ eV}$ lower than calculated energy, $\sim 1.0 \text{ eV}$ [33]. We suggest that the $\sim 0.5 \text{ eV}$ energy difference is the d - d^* exciton binding energy.

This point is further supported by reinterpreting Uchida *et al.*'s work [28,34]. In their work, it was found on the one hand that the in-plane ω_p of the over-doped samples did not increase higher than that of $p = 0.16$ (actually it decreased slightly at $p = 0.34$) and the 0.5 eV peak in the in-plane $\sigma_1(\omega)$ loses its strength as the doping increases beyond $p = 0.16$. This observation suggests that the in-plane free carrier contribution remains fixed and the reduction in the d - d^* exciton band strength is directly resulted from the decrease of the available $d_{3z^2-r^2}$ states as carriers occupy them. On the other hand, the Drude-like peak starts to appear in the c -axis conductivity for $p > 0.16$ and yet, the corresponding c -axis plasma frequency remains small compared to the in-plane one. We believe that the systematic decrease in the resistivity (both in-plane and c -axis) with doping is due to the three-dimensional crossover.

4. Summary and Conclusion

We have demonstrated that the high T_c cuprate physics has its foundation on the Wigner lattice ground state order away from half-filling. We observed a clear indication of the competition between two Wigner lattice orders, one corresponds to a $T_c = 15 \text{ K}$ and the other to $T_c = 30 \text{ K}$. We were able to explain the metallic transport in 1% Sr-doped La_2CuO_4 . Based on our findings, a new type of I-M transition mechanism has been established. The observed phase collective mode in the SC state provides a channel for the coupling of the c -axis polarized far-IR photon field to the fluctuations of the relative phase between the SC condensate and the Wigner lattice

order.

Acknowledgement We would like to thank Zugang Li, Zheng Wu and Young Seok Song for their various technical assistance as well as sample preparations and characterizations. We also thank John Markus for his technical helps to expedite our experiment. One of us (P.H.H.) is supported by the State of Texas through the Texas Center for Superconductivity at the University of Houston.

REFERENCES

1. See for example, T.M. Rice, *Physica C* 282-287, xix-xxiii (1997); B. Batlogg, *Physica C* 282-287, xxiv-xxx (1997).
2. Y.H. Kim and P.H. Hor, *Mod. Phys. Lett. B* 15, 497 (2001).
3. (a) D.J.C. Walker, A.P. Mackenzie, and J.R. Cooper, *Phys. Rev. B* 51, 15653; (b) Y. Fuzukumi, K. Mizuhashi, K. Takenaka, and S. Uchida, *Phys. Rev. Lett.* 76, 684 (1996); (c) G.S. Boebinger, Y. Ando, A. Passner, T. Kimura, M. Okuya, J. Shimoyama, K. Kishio, K. Tamasaku, N. Ichikawa, and S. Uchida, *Phys. Rev. Lett.* 77, 5417 (1996).
4. Y. Ando, A.N. Lavrov, S. Komiya, K. Segawa, and X.F. Sun, *Phys. Rev. Lett.* 87, 017001 (2001).
5. T. Kakeshita, S. Uchida, K.M. Kojima, S. Adachi, S. Tajima, B. Gorshunov, and M. Dressel, *Phys. Rev. Lett.* 86, 4140 (2001); D. Dulic, A. Pimenov, D. van der Marel, D.M. Broun, S. Kamal, W.N. Hardy, A.A. Tsetkov, I.M. Sutjaha, R. Liang, A.A. Menovsky, A. Loidl, and S.S. Saxena, *Phys. Rev. Lett.* 86, 4144 (2001).
6. D.C. Johnston, *Phys. Rev. Lett.* 62, 957 (1989).
7. T. Timusk and B. Statt, *Rep. Prog. Phys.* 62, 61 (1999).
8. Actual m^* should be larger because the underestimation of the reflectivity for $\omega > 400 \text{ cm}^{-1}$, which is inherent to the polycrystalline nature of the sample.
9. A. Dahm and W.F. Vinen, *Physics Today*, February Issue (1987), p43.
10. S.V. Kravchenko, G.V. Kravchenko, J.E. Furneaux, V.M. Pudalov, and M. D'Iorio, *Phys. Rev. B* 50, 8039 (1994).
11. J. Yoon, C.C. Li, D. Shahar, D.C. Tsui, and M. Shayegan, *Phys. Rev. Lett.* 82, 1744 (1999).
12. B. Tanatar and D.M. Ceperley, *Phys. Rev. B* 39, 5005 (1989).
13. S.T. Chui and B. Tanatar, *Phys. Rev. Lett.* 74, 458 (1995).
14. L. Bonsall and A.A. Maradudin, *Phys. Rev. B* 15, 1959 (1977).
15. Y.H. Kim, A.J. Heeger, L. Acedo, G. Stucky, and F. Wudl, *Phys. Rev. B* 36, 7252 (1987); Y.H. Kim, S-W. Cheong, and Z. Fisk, *Phys. Rev. Lett.* 67, 2227 (1991).
16. P.H. Hor et al., to be published.
17. V.J. Emery and S.A. Kivelson, *Nature* 374, 434 (1995).
18. J. Corson, R. Mallozzi, J. Orenstein, J.N. Eckstein, and I. Bozovic, *Nature* 398, 221 (1999).
19. Z.A. Xu, N.P. Ong, Y. Wang, T. Takeshita, and S. Uchida, *Nature* 406, 486 (2000).
20. Y. Nambu, *Phys. Rev.* 117, 648 (1960).
21. Actual γ should be smaller than estimated $\gamma \sim 0.2$ for $p = 0.07$ with $m^* \sim 40 m_e$ because of the aforementioned underestimation of m^* .
22. A.J. Leggett, *Prog. Theor. Phys.* 36, 901 (1966).
23. K. Tamasaku, Y. Nakamura, and S. Uchida, *Phys. Rev. Lett.* 69, 1455 (1992).
24. J.H. Kim, H.S. Somal, M.T. Czyzk, D. van der Marel, A. Wittlin, A.M. Gerrits, V.H.M. Dujin, N.T. Hien, and A.A. Menovsky, *Physica C* 247, 297 (1995).
25. C.C. Homes, T. Timusk, R. Liang, D.A. Bonn, and W.N. Hardy, *Phys. Rev. Lett.* 71, 1645 (1993).
26. T. Motohashi, J. Shimoyama, K. Kitazawa, K. Kishio, K.M. Kojima, S. Uchida, S. Tajima, *Phys. Rev. B* 61, 9269 (2000).
27. D.N. Basov, H.A. Mook, B. Dabrowski, and T. Timusk, *Phys. Rev. B* 52, 13141 (1995).
28. S. Uchida, T. Ido, H. Takagi, T. Arima, Y. Tokura, and S. Tajima, *Phys. Rev. B* 43, 7942 (1991).
29. F. Gao, D.B. Romero, D.B. Tanner, J. Talvacchio, and M.G. Forrester, *Phys. Rev. B* 47,

- 1036 (1993).
30. M.A. Quijada, D.B. Tanner, F.C. Chou, D.C. Johnston, S.-W. Cheong, Phys. Rev. B52, 15485 (1995).
 31. D.B. Tanner, F. Gao, K. Kamaras, H.L. Liu, M.A. Quijada, D.B. Romero, Y.-D. Yoon, A. Zibold, H. Berger, G. Margaritondo, L. Forro, R.J. Kelly, M. Onellion, G. Cao, J.E. Crow, B.H. O, J.T. Markert, J.P. Rice, D.M. Ginzberg, and Th. Wolf, Physica C341-348, 2193 (2000).
 32. Z. G. Li and P. H. Hor in Stripe and Related Phenomena, ed. Bianconi and Saini, (Kluwer Academic/Plenum Publishers, New York, 2000), p515.
 33. J.D. Perkins, R.J. Birgeneau, J.M. Graybeal, M.A. Kastner, and D.S. Kleinberg, Phys. Rev. B58, 9390 (1998) and references therein.
 34. S. Uchida, K. Tamasaku, and S. Tajima, Phys. Rev. B53, 14558 (1996).